International Journal of Engineering Research & Technology (IJERT)
ISSN: 2278-0181
Vol. 5 Issue 06, June-2016

Numerical Analysis of Gas Tungsten Arc Welded AISI 316LN Austenitic Stainless Steel Joints using Response Surface Methodology and Finite Element Anlysis

C. R. Ashwin Kumar,
PG Scholar,
Dept. of Mechanical Engineering,
Sri Ramanujar Engineering College,
Chennai-600 127, India,

Dr. S. Sathiyamurthy,
Professor and Dean,
Dept. of Mechanical Engineering,
Sri Ramanujar Engineering College,
Chennai-600 127, India,

***Abstract*— 316LN stainless steel is majorly used in the Fast Breeder Reactors (FBR) because of its better corrosion resistance and high strength. Gas Tungsten Arc Welding (GTAW) is a potential candidate to fabricate quality weld joints. However, the process parameters should select in such a way the joints have enough penetration and smaller weld width. So it is necessary to understand the effect of process parameters on the weld penetration and width. Hence in this investigation the process parameters namely current, welding speed and gas and flow rate on weld bead geometry was studied. The response surface methodology is employed to develop the empirical relationship to predicted the penetration and weld width. Using the FE numerical data generated on the influence of process variables on weld-bead geometry, regression models correlating the weld-bead shape parameters with the process parameters were developed for determining the objective function in response surface methodology (RSM). Experimental validation was carried out to verify the optimized weld joint. Close agreement was achieved between the experimental weld-bead profile and the optimized weld-bead profile.**

Keywords*— Gas tungsten arc welding; stainless steel; Response surface methodology); finite element analysis

I. INTRODUCTION

Austenitic stainless steels are widely used in many industries utilizing high temperature components such as heat exchangers and chemical reactors, because of their good mechanical properties at elevated temperatures and their excellent corrosion resistance [1]. While these alloys have useful properties in the wrought condition, welding is known to deteriorate its properties by following three ways. Three main problems encountered in the welding of austenitic stainless steel stand out. These are sensitive structure developing after the formation of chromium carbide on the surface that is being heated, the formation of hot fracture, and the formation of sigma phase risks encountered at high working temperatures [2, 3]. Yousefieh et al made an investigation on the effect of heat input on the microstructural characteristics and corrosion properties of duplex stainless steel [4]. The study reports that change in heat input alters the bead geometry and phase compositions like sigma phase and Cr_2N phases. Mondal et al reported that weld bead quality are evaluated by bead geometry and it is solely influenced by heat input [5]. Hence Regression analysis was done on the effect of process parameters on the weld bead geometry. The study revealed that the weld bead geometry linearly related with the heat input. Similarly Almazrouee et al developed an empirical relationship between the welding parameters like amperage, the voltage, and the traverse speed, and percentage of mixed gas of GTAW of low alloy steel [6]. The study reports that the bead penetration is greatly influenced by voltage than the traverse speed whereas; the amperage has less significant on the bead geometry. In another study, Kurtulmus et al attempt an investigation on effect of welding current and arc voltage of flux core arc welding of steel [7]. The study reported that the deposition rate was increased with increase with current and decrease in voltage. The reinforcement height and the penetration increases with the amperage. Kumar et al study the effect of heat input on GTAW AISI 304 stainless steel joints [8]. The study reported that increase in heat input increases the grain size and thereby reduces the mechanical properties. From the literature, it is understood that the process parameters have greater effect in deciding the heat input and thereby microstructural characteristics and mechanical properties of the weld joints [9]. So it is necessary to understand the effect of process parameters to predict the joint performance. Hence, in this investigation, the effect of three parameters namely current, welding speed and gas flow rate on weld penetration, weld width and peak temperature of GTAW AISI 316LN stainless steel joints. In addition, the empirical relationship between the process parameters on response like weld penetration, weld width and peak temperature were developed.

II. EXPERIMENTS

In this investigation, AISI 316LN Austenitic stainless steel is used as the parent metal. The chemical composition is verified using spectro-chemical analysis and it is presented in table 1. The mechanical properties of parent metal are presented in table 2. Table 3 shows the electrode details used in this investigation. The joint configuration of 150 x 150 x 3 mm is used in this investigation. Optical microscope was employed to reveal the macrostructure of the optimum weld joint. Then weld bead width and the penetration

International Journal of Engineering Research & Technology (IJERT)
ISSN: 2278-0181
Vol. 5 Issue 06, June-2016

TABLE I. CHEMICAL COMPOSITION (WT %) OF PARENT METAL

Element	Fe	Cr	Ni	Mo	Mn	Si	C
Content	Balance	18.0	14.0	3.0	2.00	1.00	0.03

TABLE II. MECHANICAL PROPERTIES OF 316LN STAINLESS STEEL

Properties	Yield strength	Tensile strength	Poisson's ratio
Values	205 MPa	515 MPa	0.27-0.30

TABLE III. DETAILS OF ELECTRODE PARAMETERS

S.No	Parameter	GTAW
1	Electrode diameter (mm)	1.6
2	Arc gap (mm)	2

TABLE IV. IMPORTANT PROCESS VARIABLES AND THEIR WORKING LIMITS

Parameters	Levels				
	-1.68	*-1*	*0*	*1*	*1.68*
Current, I (A)	110	118	130	141	150
Welding speed, S (cm/min)	5	7	9	11	13
Gas flow rate, G (l/min)	13	14	15	16	17

III. FINITE ELEMENT ANALYSIS

This paper regards three-dimensional nonlinear thermal analysis using the finite element welding simulation code SYSWELD. The meshed model composed of dissimilar elements ranges from triangular, quadralateral and rectangular elements. The gradient meshed model of 18479 elements used for finite element analysis is depicted in (Fig.1). Fine meshing was carried out near the weld region and heat affected zone to achieve the accruate results. Whereas, coarse meshing was carriedout outer regions in order to reduce the computational time. The thermal analysis was carried out to predict the temperature distribution and to predict the peak temperature.

A. Thermal Boundary Condition

The governing differential equation for three dimensional heat conduction equations for a solid in cartesian coordinate system is given by

$$\frac{\delta}{\delta x}\left(k_x \frac{\delta T}{\delta x}\right)+\frac{\delta}{\delta y}\left(k_y \frac{\delta T}{\delta y}\right)+\frac{\delta}{\delta z}\left(k_z \frac{\delta T}{\delta z}\right)+q_g=\rho C\left(\frac{\delta T}{\delta t}\right) \quad (1)$$

Where, thermal diffusivity of the material, q_g is the heat generation per unit volume in W/m^3, ρ is density of the material in kg/m^3; Cp is specific heat in J/kgK and kx, ky, kz are thermal conductivity W/mK. At the solid boundary, by Newton's law of heating and cooling, convective heat is given as

$$-k\frac{dT}{dx}=h_c(T_s-T_\infty) \quad (2)$$

Where h_c includes the convective and radioactive heat transfer and calculated by empirical relationship, at all free surfaces

$$h_c=2.41x10^{-3}\varepsilon T^{1.61} \quad (3)$$

Where ε is emissivity, T is temperature (K), Ts is surface temperature (K), and T_∞ is ambient temperature (K).

A temperature based material properties are considered for the finite element analysis. Thermal boundary conditions are symmetrical across the weld centerline. Heat transfer from the workpiece to the clamp is negligible, thus heat conducted to clamp is not accounted in this investigation.

B. Mechanical Boundary Conditions

Zero displacement conditions were used for constraining the butt joint which resembling the complete fixed fixturing. The mid-plane of the butt joint is assumed to be a plane of symmetry in the analysis, which is parallel to the y-z plane.

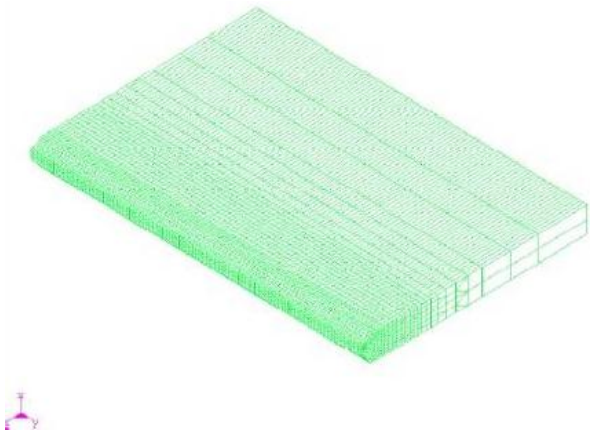

Fig.1 Meshed model

IV. RESULTS AND DISCUSSION

A. Working Limits of Parameters

The working limits for RSM technique is selected based on conducting many trail experiments. The visual inspection method was employed to identify the quality of the weld joint. In addition the optical microscope was employed to find the extent of penetration. The non-destructive tests were used to identify the working limits of the welding parameters. The results obtained are as following. If the current is less than 110 A, there will be incomplete penetration and lack of fusion. For current greater than 150 A, undercut and spatter will be observed on the weld bead surface. If the welding speed is lower than 5 cm/min, undercut will be observed due to increased heat input. For welding speed greater than 13 cm/min, there will be lack of fusion and lack of penetration. If the flow rate of shielding gas is lower than 13 l/min, porosities and tungsten inclusions will be observed and flow rate of shielding gas greater than 17 l/min will lead to the generation of porosities due to agitated flow gas. The finding of working limits allows achieving the defect free sound joints. Within the selected range of parameters, five levels of value were chosen for the design of central composite matrix. In this investigation, three factors, five level was used for the optimization of process parameters.

Table 3 lists the range of selected parameters and Fig. 2 shows 20 sets of coded conditions used to establish the design matrix. Considering the convenience of recording and processing experimental data, upper and lower levels of the parameters were coded as +1.682 and -1.682, respectively [10].

International Journal of Engineering Research & Technology (IJERT)
ISSN: 2278-0181
Vol. 5 Issue 06, June-2016

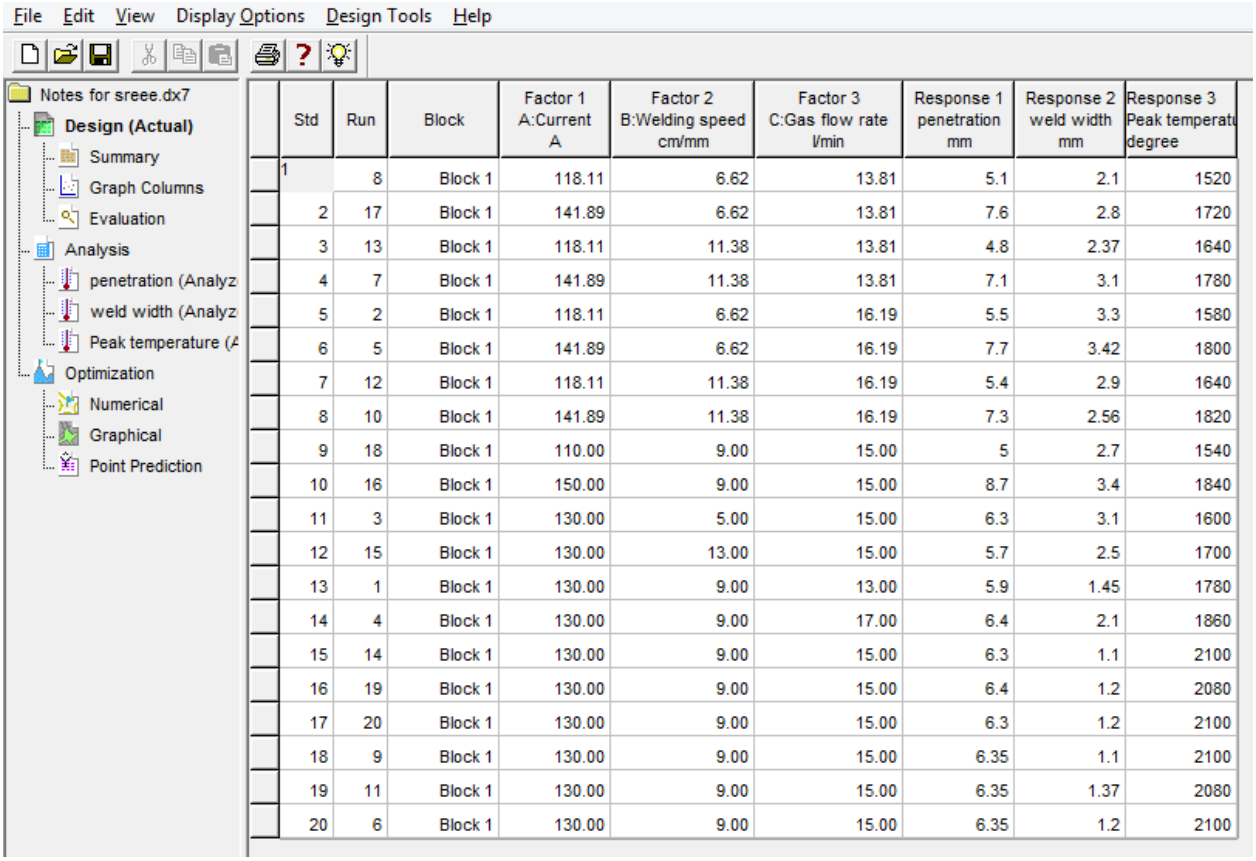

	Std	Run	Block	Factor 1 A:Current A	Factor 2 B:Welding speed cm/mm	Factor 3 C:Gas flow rate l/min	Response 1 penetration mm	Response 2 weld width mm	Response 3 Peak temperatu degree
1	8	Block 1	118.11	6.62	13.81	5.1	2.1	1520
2	17	Block 1	141.89	6.62	13.81	7.6	2.8	1720
3	13	Block 1	118.11	11.38	13.81	4.8	2.37	1640
4	7	Block 1	141.89	11.38	13.81	7.1	3.1	1780
5	2	Block 1	118.11	6.62	16.19	5.5	3.3	1580
6	5	Block 1	141.89	6.62	16.19	7.7	3.42	1800
7	12	Block 1	118.11	11.38	16.19	5.4	2.9	1640
8	10	Block 1	141.89	11.38	16.19	7.3	2.56	1820
9	18	Block 1	110.00	9.00	15.00	5	2.7	1540
10	16	Block 1	150.00	9.00	15.00	8.7	3.4	1840
11	3	Block 1	130.00	5.00	15.00	6.3	3.1	1600
12	15	Block 1	130.00	13.00	15.00	5.7	2.5	1700
13	1	Block 1	130.00	9.00	13.00	5.9	1.45	1780
14	4	Block 1	130.00	9.00	17.00	6.4	2.1	1860
15	14	Block 1	130.00	9.00	15.00	6.3	1.1	2100
16	19	Block 1	130.00	9.00	15.00	6.4	1.2	2080
17	20	Block 1	130.00	9.00	15.00	6.3	1.2	2100
18	9	Block 1	130.00	9.00	15.00	6.35	1.1	2100
19	11	Block 1	130.00	9.00	15.00	6.35	1.37	2080
20	6	Block 1	130.00	9.00	15.00	6.35	1.2	2100

Fig. 2. Design matrix

The adequacy of the framed relationship was tested using the analysis of variance technique (ANOVA) [11]. In this methodology, if the calculated 'F' ratio of the developed model is less than the standard 'F' ratio (from ANOVA table) at a 95 % confidence level, the model is adequate within the confidence limit [12]. The adequate ANOVA tables of penetration, weld width and peak temperature are presented in Fig. 3.

The purpose of the ANOVA is to investigate which welding process parameters significantly affect the quality characteristics. It is understood that the developed relationship is adequate at 95% confidence level. If values of 'prob>F' are less than 0.0500, the relationship terms will be considered significant [13, 14]. In this model, I, G, S and T are significant model terms. Values greater than 0.1000 indicate that the relationship terms are not significant. Coefficient of determination 'R^2' is used to find how close the predicted and experimental values lie [15]. The value of 'R^2' for the peak temperature developed relationship is also presented in Fig 3c, which indicates high correlation exists between the experimental and predicted values. The 'R-squared' of 0.946 is in reasonable agreement with the 'adj R-squared' of 0.932.

The value of probability > F in Figs. 3a, 3b and 3c for model is less than 0.05, which indicates that the model is significant. Correspondingly, Welding current, Welding speed and Gas flow rate have significant effects. Lack of fit is non significant as it is preferred.

The influence of amperage, welding speed and gas flow rate on weld width and penetration can be explained by attained heat input. The increase in heat input increases the extent of melting and thereby the weld width and penetration increased. The insufficient heat input will reduce the extent of melting and thereby it resulted in lower weld width and poor penetration. If the heat input is excess, the weld width is larger and burn-off may occur. So it is necessary to attain the optimum heat input to achieve the less weld width with full penetration. Conventionally the heat input is calculated using the relationship ((voltage x current)/welding speed) which represent the energy by unit of length.

Thus, it governs the heat transferred (thermal cycles), geometry and inturn affects the microstructure and then the hardness of the weld. Too low a heat input easily resulted in the presence of welding defects, which seriously decreased the strength of the welded joint. The most important characteristic of heat input is that it governs the cooling rates in welds and thereby affects the microstructure of the weld metal. A change in microstructure directly affects the mechanical properties of weld. From the design matrix, it is notable that the responses recorded show variations with respect to the change in the process parameter combinations. This represent that all the three parameters have significant effect on the responses. From the ANOVA table and design matrix it was found that welding current is the most significant process parameters deciding the weld bead geometry and temperature attained. This is attributed to the deposition rate and formation of high intense arc column.

International Journal of Engineering Research & Technology (IJERT)
ISSN: 2278-0181
Vol. 5 Issue 06, June-2016

ANOVA for Response Surface Quadratic Model
Analysis of variance table [Partial sum of squares - Type III]

Source	Sum of Squares	df	Mean Square	F Value	p-value Prob > F	
Model	18.40	9	2.04	1756.35	< 0.0001	significant
A-Current	*16.75*	*1*	*16.75*	*14385.44*	*< 0.0001*	
B-Welding spee	*0.39*	*1*	*0.39*	*335.39*	*< 0.0001*	
C-Gas flow rate	*0.34*	*1*	*0.34*	*288.31*	*< 0.0001*	
AB	*0.031*	*1*	*0.031*	*26.85*	*0.0004*	
AC	*0.061*	*1*	*0.061*	*52.62*	*< 0.0001*	
BC	*0.011*	*1*	*0.011*	*9.66*	*0.0111*	
A^2	*0.44*	*1*	*0.44*	*381.02*	*< 0.0001*	
B^2	*0.23*	*1*	*0.23*	*193.71*	*< 0.0001*	
C^2	*0.075*	*1*	*0.075*	*64.27*	*< 0.0001*	
Residual	0.012	10	1.164E-003			
Lack of Fit	*4.557E-003*	*5*	*9.115E-004*	*0.64*	*0.6799*	*not significant*
Pure Error	*7.083E-003*	*5*	*1.417E-003*			
Cor Total	18.41	19				

a. Penetration

ANOVA for Response Surface Quadratic Model
Analysis of variance table [Partial sum of squares - Type III]

Source	Sum of Squares	df	Mean Square	F Value	p-value Prob > F	
Model	13.51	9	1.50	61.73	< 0.0001	significant
A-Current	*0.42*	*1*	*0.42*	*17.16*	*0.0020*	
B-Welding spee	*0.21*	*1*	*0.21*	*8.69*	*0.0146*	
C-Gas flow rate	*0.62*	*1*	*0.62*	*25.38*	*0.0005*	
AB	*0.023*	*1*	*0.023*	*0.95*	*0.3526*	
AC	*0.34*	*1*	*0.34*	*14.00*	*0.0038*	
BC	*0.42*	*1*	*0.42*	*17.22*	*0.0020*	
A^2	*7.00*	*1*	*7.00*	*288.00*	*< 0.0001*	
B^2	*5.34*	*1*	*5.34*	*219.59*	*< 0.0001*	
C^2	*0.87*	*1*	*0.87*	*35.95*	*0.0001*	
Residual	0.24	10	0.024			
Lack of Fit	*0.19*	*5*	*0.039*	*3.99*	*0.0776*	*not significant*
Pure Error	*0.049*	*5*	*9.750E-003*			
Cor Total	13.75	19				

b. Weld width

ANOVA for Response Surface Quadratic Model
Analysis of variance table [Partial sum of squares - Type III]

Source	Sum of Squares	df	Mean Square	F Value	p-value Prob > F	
Model	8.170E+005	9	90779.93	945.03	< 0.0001	significant
A-Current	*1.134E+005*	*1*	*1.134E+005*	*1180.65*	*< 0.0001*	
B-Welding spee	*13424.58*	*1*	*13424.58*	*139.75*	*< 0.0001*	
C-Gas flow rate	*7244.54*	*1*	*7244.54*	*75.42*	*< 0.0001*	
AB	*1250.00*	*1*	*1250.00*	*13.01*	*0.0048*	
AC	*450.00*	*1*	*450.00*	*4.68*	*0.0557*	
BC	*1250.00*	*1*	*1250.00*	*13.01*	*0.0048*	
A^2	*3.017E+005*	*1*	*3.017E+005*	*3140.31*	*< 0.0001*	
B^2	*3.635E+005*	*1*	*3.635E+005*	*3784.23*	*< 0.0001*	
C^2	*1.404E+005*	*1*	*1.404E+005*	*1462.00*	*< 0.0001*	
Residual	960.60	10	96.06			
Lack of Fit	*427.27*	*5*	*85.45*	*0.80*	*0.5932*	*not significant*
Pure Error	*533.33*	*5*	*106.67*			
Cor Total	8.180E+005	19				

c. Peak Temperature

Fig. 3. ANNOVA table

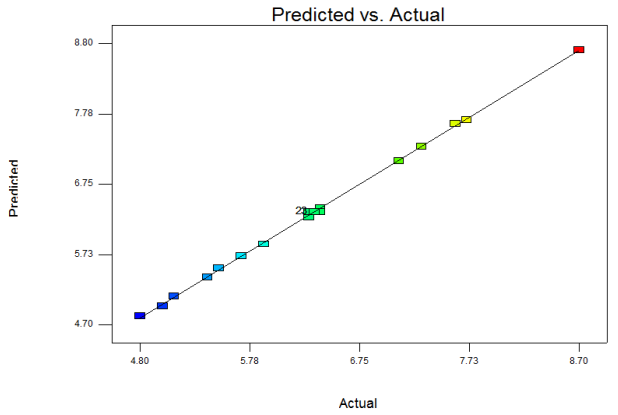

a. Penetration

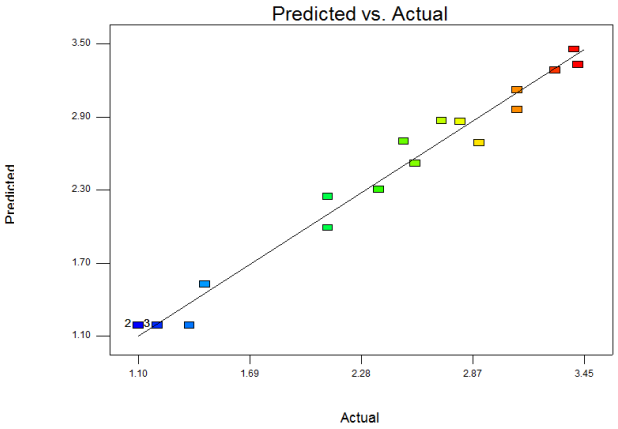

b. Weld width

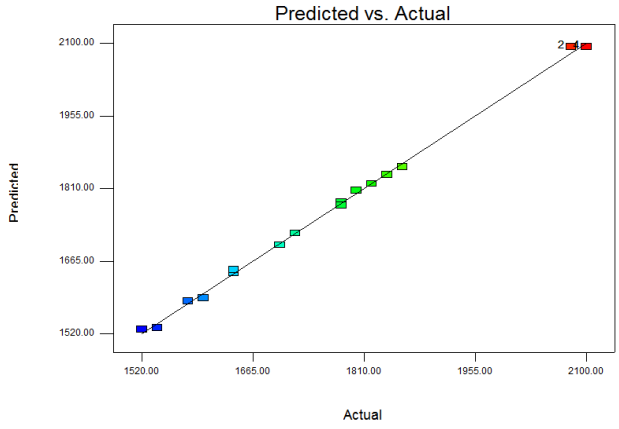

c. Peak temperature

Fig. 4. Correlation map

B. *Development of an Empirical Relationship*

Central composite design matrix results comparatively excellent calculations over the whole design domain and does not need practice of points other than the original factor domain [16]. The upper limit and lower limit of the factors were coded as +1.682 and –1.682 respectively. In this study, the response functions of the joint, weld width, penetration depth and peak temperature, are functions of current (I), welding speed (S) and flow rate of shielding gas (G), and it can be expressed in the Equation 1, 2 and 3.

After determining the significant coefficients (at 95% confidence level), the empirical relationships were developed using these coefficients [17]. The developed empirical relationships to predict penetration, weld width and peak temperature are as follows:

Penetration = -12.25103 - 0.11672 × Current + 0.41532 × Welding speed + 2.34533 × Gas flow rate - 2.20971E-003 × Current × Welding speed - 6.18718E-003 × Current × Gas flow rate + 0.013258 × Welding speed × Gas flow rate + 1.24050E-003 × Current^2 -0.022112 × Welding speed^2 - 0.050950 × Gas flow rate^2 (4)

International Journal of Engineering Research & Technology (IJERT)
ISSN: 2278-0181
Vol. 5 Issue 06, June-2016

Weld width = +86.68866 -1.03099 × Current -0.52896 × Welding speed 2.42212 × Gas flow rate -1.90035E-003 × Current × Welding speed -0.014584 × Current × Gas flow rate -0.080875 × welding speed × Gas flow rate + 4.92906E-003 × Current^2 + 0.10760 × Welding speed^2 + 0.17416 × Gas flow rate^2 (5)

Peak temperature = -34660.52649 + 269.67502 × Current + 642.29227 × Welding speed + 2084.30861 × Gas flow rate -0.44194 × Current × Welding speed + 0.53033 × Current × Gas flow rate - 4.41942 × Welding speed × Gas flow rate - 1.02304 × Current^2 -28.07591 × Welding speed^2 - 69.80364 × Gas flow rate^2 (6)

TABLE V. DESIGN CRITERIA

Name	Goal	Importance
Current (I)	is in range	3
Welding speed (S)	is in range	3
Gas flow rate (G)	is in range	3
Weld width (W)	minimize	3
Penetration (P)	maximize	3
Peak temperature (PT)	none	3

From the equations 4, 5 and 6 the weld width, penetration and peak temperature can be predicted for any number of parameter combinations within the working limit. RSM technique is employed to optimize the process parameters and the table 5 shows the design criteria used for the optimization. The parameters like current, welding speed and penetration are set as in rang. But the output response weld width assign as minimization problem because as the weld width increases, the joint properties get reduced because of the detrimental microstructures. The output response penetration is set as maximization problem, since the reduction in the weld penetration shows a gap at the root which is considered as the defect. For peak temperature, the goal is set as none.

TABLE VI. OPTIMIZED SOLUTIONS

S.No	I	S	G	P	WW	PT	Desirability
1	134.7	6.79	13	6.53297	2.149	1602.70	0.5930
2	138.6	11.13	17	6.95978	2.486	1725.14	0.5241
3	138.7	11.12	17	6.96707	2.485	1726.60	0.52418
4	138.4	11.12	17	6.94190	2.470	1728.52	0.52413
5	133.6	11.14	17	6.49722	2.276	1748.21	0.50677

From the finite element analysis the temperature attained and bead geometries were measured for the suggested combinations of process parameters. Table 6 shows the optimized solutions achieved for the proposed design criteria. Figure 4 shows the correlation plots between the predicted and actual values in which the values were fit. However, the optimum solution should be validated in order to know the accuracy of the model. Figure 5 shows the FEA results for the optimized result. Figure 5a shows the 3-dimensional temperature contour map which shows that the maximum temperature was recorded in the weld center and the temperature is gradually reduced from the weld centerline. Figure 5b shows the cross sectional thermal map which shows the thermal gradients. The red color represent the weld region which attain the region attain above the melting temperature. The region next to weld region represents the partially melted zone which is shown in orange color. It was confirmed that the usage of optimized process parameter results in low weld width with sufficient penetration.

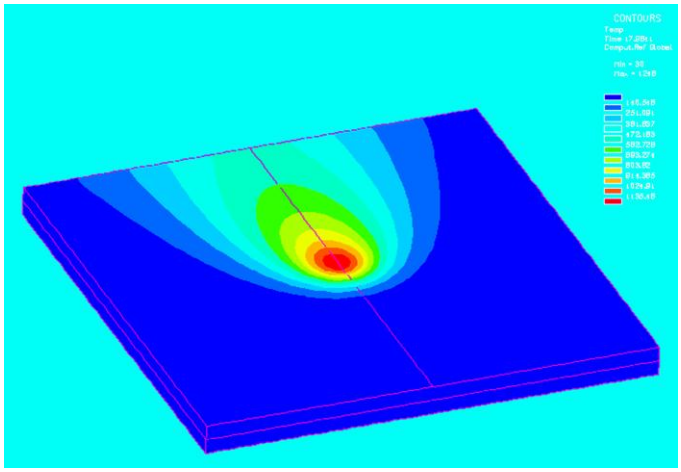

a. 3D thermal contour map

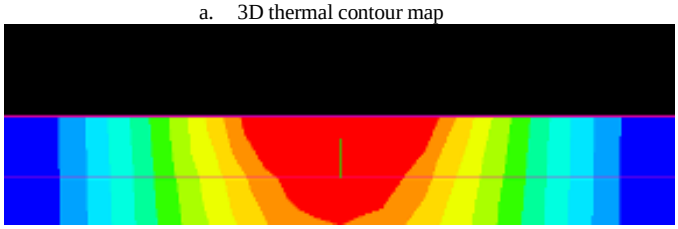

b. Cross sectional contour map

Fig 5 FEA results

a. Macrographs

b. Weld face

c. Weld root

Fig 6 Experimental validation

Figure 6 shows the experimental validation of the optimized joint. The results once again confirm the accuracy of the optimized and FEA results holds good. Figure 6a shows the macrographs of the joint in which the shape of the weld zone is shows good agreement with the FEA results. Figure 6b and 6c shows the photographs of weld face and weld root. The weld face is free from defects like undercuts, spatters and cracks. Similarly the weld root is free from root defects like insufficient penetration.

International Journal of Engineering Research & Technology (IJERT)
ISSN: 2278-0181
Vol. 5 Issue 06, June-2016

V. CONCLUSIONS

From the investigation following conclusions were framed:

1. Empirical relationships are developed using design of experiments and analysis of variance to predict the penetration, weld width and peak temperature of GTA welded stainless steel joints at 95% confidence level.
2. The optimized parameters were predicted and the results were validated using FEA and experimental method which shows good agreement.

REFERENCES

[1]. P.K. Palani, and N. Murugan, "Optimization of weld bead geometry for stainless steel claddings deposited by FCAW", J. Mater. Proces. Tech., vol. 190, pp. 291-299, 2007.

[2]. K.Y. Benyounis, A.G. Olabi, M.S.J Hashmi, "Multi-response optimization of CO2 laser-welding process of austenitic stainless steel", Optics Laser Tech, vol. 40, pp. 76-87, 2008.

[3]. M. Balasubramanian, M. Jayabalan and V. Balasubramanian, "Developing mathematical models to predict tensile properties of pulsed current gas tungsten arc welded Ti-6Al-4V alloy". Mater. Des., vol. 29(1), pp 92-97, 2008.

[4]. M. Yousefieh , M. Shamanian and A. Saatchi, "Influence of Heat Input in Pulsed Current GTAW Process on Microstructure and Corrosion Resistance of Duplex Stainless Steel Welds". J. Iron Steel Res. Int., Vol. 18 (9), pp 65-69, 2011.

[5] Ajit Mondal, Manas Kumar Saha, Ritesh Hazra and Santanu Das, "Influence of heat input on weld bead geometry using duplex stainless steel wire electrode on low alloy steel specimens", 10.1080/23311916.2016.1143598, 2016.

[6] A. Almazrouee, T. Shehata and S. Oraby "Effect of Welding Parameters on the Weld Bead Geometry of Low Alloy Steel using FCAW – Empirical Modeling Approach". Int. J. Mining, Metallurgy & Mech. Engg., Vol. 3(3), pp.88-92, 2015.

[7] Memduh Kurtulmus, Ahmet İrfan Yukler, Mustafa Kemal Bilici and Zarif Catalgol, "Effects of welding current and arc voltage on fcaw weld bead geometry", Int J Res. Engg Technol., Vol. 4(9), 2015.

[8] Subodh Kumar, A.S. Shahi, Effect of heat input on the microstructure and mechanical properties of gas tungsten arc welded AISI 304 stainless steel joints, Materials & Design, Volume 32, Issue 6, June 2011, Pages 3617–3623

[9]. Bor-Tsuen Lin, Ming-Der Jean and Jyh-Horng Chou, "Using response surface methodology with response transformation in optimizing plasma spraying coatings", J. Adva. Manu. Tech, vol. 34, pp. 307-315, 2007.

[10]. G.E.P. Box, W.G.Hunter, and J.S. Hunter, "Statistics for Experimenters: An Introduction to Design", Data Analysis, and Model Building, John Wiley and Sons, 1978.

[11]. Johnson and F.C. Leona F.C., "Statistics and Experimental Design in Engineering and Physical Sciences", vol.2, John Wiley & sons, New York, 1964.

[12]. J.E. Miller, Freund and R. Johnson, "Probability and Statistics for Engineers", vol.5, Prentice Hall, New Delhi, 1996.

[13]. E. Vincent Cangelosi, H. Phillip Taylor and F. Philip Rice, Basic statistics: A real world approach, 43rd ed, West publishing company 1983.

[14]. V. Gunaraj and N. Murugan, "Application of response surface methodology for predicting weld bead quality in submerged arc welding of pipes", J. Mater. Process. Tech., vol. 88, pp. 266-275, 1999.

[15]. K. Manonmani, N. Murugan and G. Buvanasekaran, "Effect of process parameters on the weld bead geometry of laser beam welded stainless steel sheets", Inter. J. Joining Materials, vol. 17(4), pp.103-109, 2005.

[16]. Tung-Hsu Hou, Chi-Hung Su and Wang-Lin Liu, "Parameters optimization of a nano-particle wet milling process using the Taguchi method, response surface method and genetic algorithm" Powd. Tech., Vol.173, pp.153-162, 2007.

[17]. M. Jayaraman, R. Sivasubramanian, V. Balasubramanian and A.K. Lakshminarayanan, "Prediction of tensile strength of friction stir welded A356 cast aluminium alloy using response surface methodology and artificial neural network", Inter J. Manu. Sci. Prod., vol. 9(1-2), pp. 45-60, 2008.